Latest Molding Simulation and Mechanical Performance Prediction for Long Fiber Composites Using Moldex3D and Digimat

Huan-Chang Tseng

CoreTech System (Moldex3D) Co., Ltd., ChuPei City, Hsinchu, 30265, Taiwan

Abstract

Long fiber reinforced polymer (LFRP) composites offer exciting new possibilities for the green automotive industry, due to their excellent mechanical properties, advantageous weight reduction and economical fuel consumption. In practice, accurately predicting fiber orientation is a critical issue in causing anisotropy in the mechanical properties of the LFRP parts. Recently, the **iARD-RPR** (Improved Anisotropic Rotary Diffusion model combined with a Retarding Principal Rate model) developed by **Moldex3D** has provided significant accuracy improvement to fiber orientation prediction. In addition, **Digimat** is a state-of-the-art tool for computing the mechanical performance of the fiber-reinforced thermoplastic composites. In this work, **Moldex3D** and **Digimat** were used to obtain the fiber orientation results in injection molding simulation and discuss the reinforcing ability of glass and carbon fibers for LFRP composites. Comparisons with experimental data are also presented herein.

Introduction

Fibers are routinely added to thermoplastics as fiber-reinforced composites in order to enhance mechanical performance and counter warpage deformation. Short fiber length is about 0.2–0.4 mm, while long fibers are generally longer than 1mm. The use of fiber-reinforced thermoplastics (FRT) is enjoying continued growth, especially in automotive application. Fiber orientation markedly affects the mechanical properties, namely, strength, stiffness, and impact. However, an accurate orientation prediction is a primary requirement for ensuring a complete simulation from injection molding to structural analysis.

From a microscopic view, fiber orientation states in a general fluid are complex. Over the last three decades, great efforts in fiber suspension rheology of theoretical research have succeeded in making it possible to describe the flow-induced variation in fiber orientation. Previously, the famous fiber orientation models, which contain the Folgar-Tucker model[1], the RSC (Reduced Strain Closure) model[2], and ARD (Anisotropic Rotary Diffusion) model[3], have been available in the commercial injection molding simulation software, ASMI (Autodesk Simulation Moldflow Insight). Significantly, the Pacific Northwest National Laboratory (PNNL) and the Oak Ridge National Laboratory (ORNL)[4] have actively integrated the predictive orientation and engineering tools for injection-molded fiber composites. According to the disclosed PNNL-ORNL report, the use of the midplane-mesh (2.5D model) versions of ASMI with the ARD-RSC could obtain good agreement of fiber orientation between the experiments and the predictions regarding fiber composites in injection molding simulation. Regrettably, the ARD-RSC model used in the 3D numerical computation resulted in inaccurate predictions.

Based on the ARD-RSC[3], Tseng *et al.*[5] developed the iARD-RPR model (known as the

Improved Anisotropic Rotary Diffusion model combined with Retarding Principal Rate model) which is suitable for predicting the core-shell orientation structure of both short and long fiber-filled materials. The iARD-RPR model has proven capable of describing anisotropic fiber orientation; as a result, it has been incorporated into the commercial software utilized for injection molding simulation, Moldex3D. Using the Solid Mesh Model based on the 3D Finite Volume Method (3D-FVM) technology, **Moldex3D** can provide the transient flow field simulation involving complex 3D geometry, complimented by its robustness and efficiency. In the Manufacturing Systems Research Lab of General Motors (GM) Research and Development, Foss *et al.*[6] utilized **Moldex3D** to investigate the short-glass-fiber orientation predictions with injection-molding simulation. Their predicted orientation distribution exhibited a reliable, classic, laminar structure: skin-shell-core-shell-skin.

Most researchers are interested in the dramatic changes of orientation states with respect to different types of fibers involving glass and carbon fibers. However, few studies on numerical simulations have attempted to demonstrate the reinforcing ability of glass/carbon fibers. In the present study, we therefore aimed to perform accurate fiber orientation prediction via the iARD-RPR model implemented with the **Moldex3D** injection molding simulation. These predicted orientation distributions are compared to the related experimental data. Moreover, we explore the dramatic changes in fiber orientation with various fiber properties under the same fiber concentration and the same matrix resin. In addition, the predicted fiber orientation is provided to estimate the tensile modulus and stress-strain response via a material modeling technology of **Digimat**.

Background of Theory

FRT melt is a concentrated suspension mixture, consisting of a fiber and polymer matrix, and is assumed to be a Generalized Newtonian Fluid (GNF). As below, we give only a brief description of theoretical basis for the sake of completeness, involving the flow governing equations and the iARD-RPR fiber orientation model.

I. Flow governing equations

A set of governing equations to describe the transient and non-isothermal fluid behaviors for channel flowing and mold filling are addressed, as below:

$$\frac{\partial \rho}{\partial t} + \nabla \cdot \rho \mathbf{u} = 0 , \tag{1}$$

$$\frac{\partial}{\partial t}(\rho \mathbf{u}) + \nabla \cdot (\rho \mathbf{u}\mathbf{u} - \boldsymbol{\sigma}) = \rho \mathbf{g} , \tag{2}$$

$$\boldsymbol{\sigma} = -P\mathbf{I} + \eta(\nabla \mathbf{u} + \nabla \mathbf{u}^{\mathrm{T}}) , \tag{3}$$

$$\rho C_P \left(\frac{\partial T}{\partial t} + \mathbf{u} \cdot \nabla T \right) = \nabla \cdot (k \nabla T) + \eta \dot{\gamma}^2 , \tag{4}$$

where ρ is density; $\mathbf{u}$ is velocity vector; t is time; $\boldsymbol{\sigma}$ is total stress tensor; $\mathbf{g}$ is acceleration vector of gravity; p is pressure; η is viscosity; C_p is specific heat; T is temperature; k is thermal conductivity; $\dot{\gamma}$ is shear rate. The true 3D Finite Volume Method (FVM), due to its robustness

and efficiency, is employed to solve the complex transient flow field in a 3D geometry.

II. The iARD-RPR fiber orientation model

A *single* fiber is regarded as an axisymmetric bond with rigidness. The bond's unit vector **p** along its axis direction can describe fiber orientation. Orientation state of a *group* of fibers is given by second moment tensor,

$$\mathbf{A} = \oint \psi(\mathbf{p})\mathbf{pp}\,d\mathbf{p}\,, \tag{5}$$

where $\psi(\mathbf{p})$ is the probability density distribution function over orientation space.

Tensor $\mathbf{A}_4$ is a fourth order orientation tensor, defined as:

$$\mathbf{A}_4 = \oint \psi(\mathbf{p})\mathbf{pppp}\,d\mathbf{p}\,, \tag{6}$$

where this tensor is also symmetric. The acceptable calculation is obtained through the eigenvalue-based optimal fitting approximation of the orthotropic closure family.

Recently, Tseng *et al.* developed the new three-parameter fiber orientation model to couple with Jeffery's hydrodynamic (HD) model, namely, the Improved Anisotropic Rotary Diffusion model combined with Retarding Principal Rate model (iARD-RPR), which is suitable for both short and long fiber-filled materials,

$$\dot{\mathbf{A}} = \dot{\mathbf{A}}_{\mathrm{HD}} + \dot{\mathbf{A}}_{\mathrm{iARD}}(C_I, C_M) + \dot{\mathbf{A}}_{\mathrm{RPR}}(\alpha)\,, \tag{7}$$

where $\dot{\mathbf{A}}$ represents the material derivative of **A**. Parameters C_I and C_M describe the fiber-fiber interaction and fiber-matrix interaction, while parameter α can slow down a response of fiber orientation. *Details of the RPR model and the iARD model are available elsewhere*[5].

First, the Jeffery term is

$$\dot{\mathbf{A}}_{\mathrm{HD}} = (\mathbf{W}\cdot\mathbf{A} - \mathbf{A}\cdot\mathbf{W}) + \xi(\mathbf{D}\cdot\mathbf{A} + \mathbf{A}\cdot\mathbf{D} - 2\mathbf{A}_4 : \mathbf{D})\,, \tag{8}$$

where **W** and **D** are vorticity tensor and rate-of-deformation tensor, respectively. ξ is the shape factor of a particle.

Second, it is significant that the rotary diffusion tensor $\mathbf{D}_r$ depends on the square of the objective rate-of-deformation tensor for defining a new iARD model[5], as below:

$$\dot{\mathbf{A}}^{\mathrm{iARD}} = \dot{\gamma}[2\mathbf{D}_r - 2\mathrm{tr}(\mathbf{D}_r)\mathbf{A} - 5\mathbf{D}_r\cdot\mathbf{A} - 5\mathbf{A}\cdot\mathbf{D}_r + 10\mathbf{A}_4 : \mathbf{D}_r] \tag{9}$$

$$\mathbf{D}_r = C_I(\mathbf{I} - C_M\frac{\mathbf{D}^2}{\left\|\mathbf{D}^2\right\|}) \tag{10}$$

where **D** is the symmetric part of the velocity-gradient tensor **L**, $\mathbf{D} = \frac{1}{2}(\mathbf{L}^{\mathrm{T}} + \mathbf{L})$. The scalar $\left\|\mathbf{D}^2\right\| = \sqrt{\frac{1}{2}\mathbf{D}^2 : \mathbf{D}^2}$ is the norm of tensor $\mathbf{D}^2$.

Eventually, the RPR model is introduced as:

$$\dot{\mathbf{A}}^{\mathrm{RPR}} = -\mathbf{R}\cdot\dot{\mathbf{\Lambda}}^{\mathrm{IOK}}\cdot\mathbf{R}^{\mathrm{T}} \tag{11}$$

$$\dot{\Lambda}_{ii}^{\mathrm{IOK}} = \alpha\dot{\lambda}_i\,,\quad i,j,k = 1,2,3 \tag{12}$$

where $\dot{\mathbf{\Lambda}}^{\mathrm{IOK}}$ is the material derivative of a particular diagonal tensor and its superscript indicates

the intrinsic orientation kinetics (IOK) assumption[7]; $\mathbf{R}$ is the rotation matrix and $\mathbf{R}^{\mathrm{T}}$ is the transpose of $\mathbf{R}$; λ_i is the eigenvalues of $\mathbf{A}$, $\lambda_1 \geq \lambda_2 \geq \lambda_3$; and $\mathbf{R}=[\mathbf{e}_1,\mathbf{e}_2,\mathbf{e}_3]$ is defined by eigenvector columns of $\mathbf{A}$.

In summary, the iARD-RPR model has only the three physical parameters: a fiber-fiber interaction parameter C_I, a fiber-matrix interaction parameter C_M and a slow-down parameter α. The iARD-RPR model has been implemented in the commercial injection molding simulation software, Moldex3D (CoreTech System Co. of Taiwan), to allow for the fiber orientation predictions. Accordingly, predictions of the fiber orientation model are contingent on the method and assumptions of the underlying numerical modeling during the mold filling.

Results and Discussion

In the present study, we used Moldex3D to simulate injection molding of an end-gated plaque for a variety of fiber composites, and to predict the fiber orientation distribution with the use of the iARD-RPR model. These accurate orientation predictions, provided to a micromechanical material modeling software, Digimat-MF, enables the computation of the mechanical performance of the fiber-reinforced thermoplastic composites. Thus, the primary objective is to explore important issues from comparisons of the results of the experiments and simulations, such as the effects of glass and carbon fibers on the mechanical performance of the FRT products.

Under the same fiber concentration of 50wt% and matrix resin of Polyamide66 (PA66), two commercial composites were used in this work: (i) 50wt% long-glass-fiber reinforced PA66 (50wt% LGF/PA66) with the Dupont grade names, Zytel-75LG50HSL-BK031; (ii) 50wt% long-carbon-fiber reinforced PA66 (50wt% LCF/PA66) with the PlastiComp grade names, Complēt® LCF50-PA66. The long glass and carbon lengths are over 1 mm and 2mm, respectively. The carbon fiber diameter is about 7μm. All of the material properties regarding the shear viscosity flow curve, PVT diagram, specific heat and thermal conductivity can be referred to elsewhere[8].

In reference to the disclosed articles[9-11], the used materials were injection-molded in the end-gated plaques, as shown in **Figure 1**: the Dupont 50wt% LGF/PA66 in the ISO 300mm x 300mm x 3mm plaque; and the PlastiComp 50wt% LCF/PA66 in the PNNL 178mm x 178mm x 3.125mm plaque. In the 2.5D (or mid-plane mesh) injection molding simulation, Phelps[9] and Jin *et al.*[10] carried out long glass fiber orientation predictions of the Dupont 50wt% LGF/PA66 composite in the ISO plaque. According to the disclosed PNNL project, Nguyen *et al.*[11] reported on the long carbon fiber orientation distribution of the PlastiComp 50wt% LCF/PA66. The molten plastic is injected from the injector nozzle and will go through a runner and a gate to fill up the cavity. For the processing conditions, the filling time, mold temperatures and melting temperatures are listed in **Table I**. There is one region marked in the center of the plaque for measuring the fiber orientation distribution across the thickness.

I. Validation of fiber orientation

Herein, Moldex3D was adopted to perform the 3D injection molding simulation and fiber orientation predictions. Hexagonal-type (Hexa) elements were used to model the plaque. The initial orientation condition at the runner entrance was set to be an isotropic state. It was

unnecessary to give an inlet condition of the experimental fiber orientation distribution set around a gate, due to the higher 3D numerical resolution and the solid runner system's considerations in the computation.

Fine-tuning the parameters is important in the fiber orientation computation. The iARD-RPR model has only the three physical parameters limited in: $0 < C_I < 0.1$, $0 < C_M < 1$, $0 < \alpha < 1$. The shell-orientation layer depends on the iARD parameters, while the core width and skin layer are controlled by the RPR parameters. According to these criteria, we can fine-tune three parameters to obtain an accurate orientation prediction by determining an optimal set of parameters. Thus, it is important to determine the optimal iARD-RPR parameters of these fiber composites.

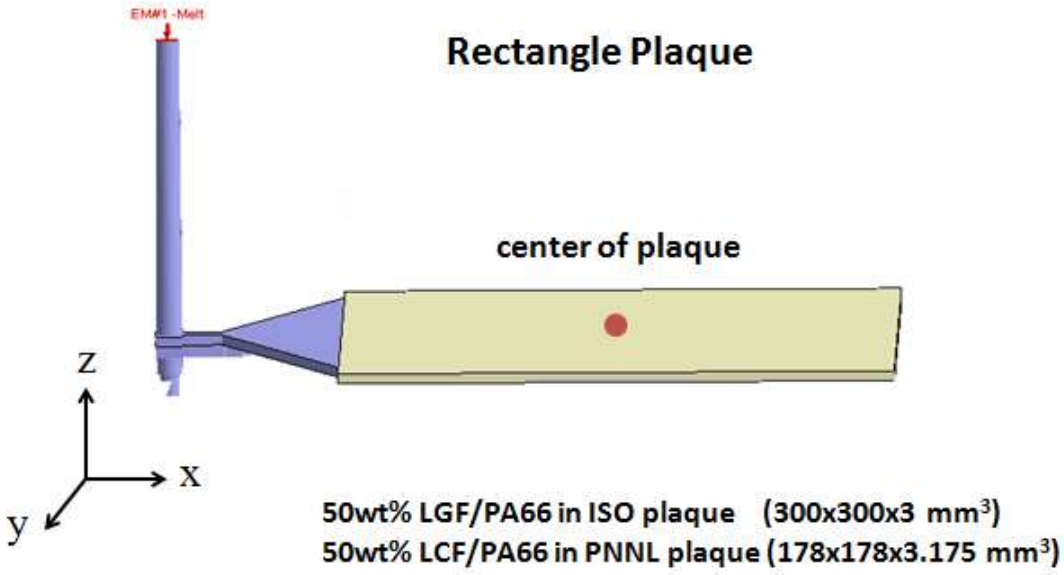

Figure 1: Geometry of the end-gated plaque in injection-molding simulations with one region measured at the center of the plaque.

Table I: Injection molding conditions for the different materials.

	50wt% LGF/PA66	*50wt% LCF/PA66*
Plaque size (mm^3)	300x300x3	178x178x3.175
Injection time (sec)	1.2	0.3
Mold temperatures (°C)	71	55
Melting temperatures (°C)	237	230

As a result, **Figures 2 and 3** show the gap-wise fiber orientation distribution across the normalized thickness at the center of the plaque for Dupont 50wt% LGF/PA66, and PlastiComp 50wt% LCF/PA66 composites, respectively. Note that A_{11} and A_{22} are defined as the flow-direction (*x*-axis) and the cross-flow-direction (*y*-axis) orientation tensor components. Fibers in the shell layers were more aligned with the flow direction, characterized by the large values of A_{11} and the low values of A_{22}; whereas, the core layer was quite wide, with low values of A_{11} and high values of A_{22}, representing the cross-flow orientation state. In the shell layer, the fibers were oriented near the walls in the flow direction by the shear deformations, which were maximal; the others were oriented in the core, wherein the deformations were weak. As shown in the figures, the fiber orientation distributions exhibited a shell–core–shell structure according to the experimental points (*see* square symbols). Overall, it appears that all of the predictive curves derived by both models were in good agreement with the experimental data.

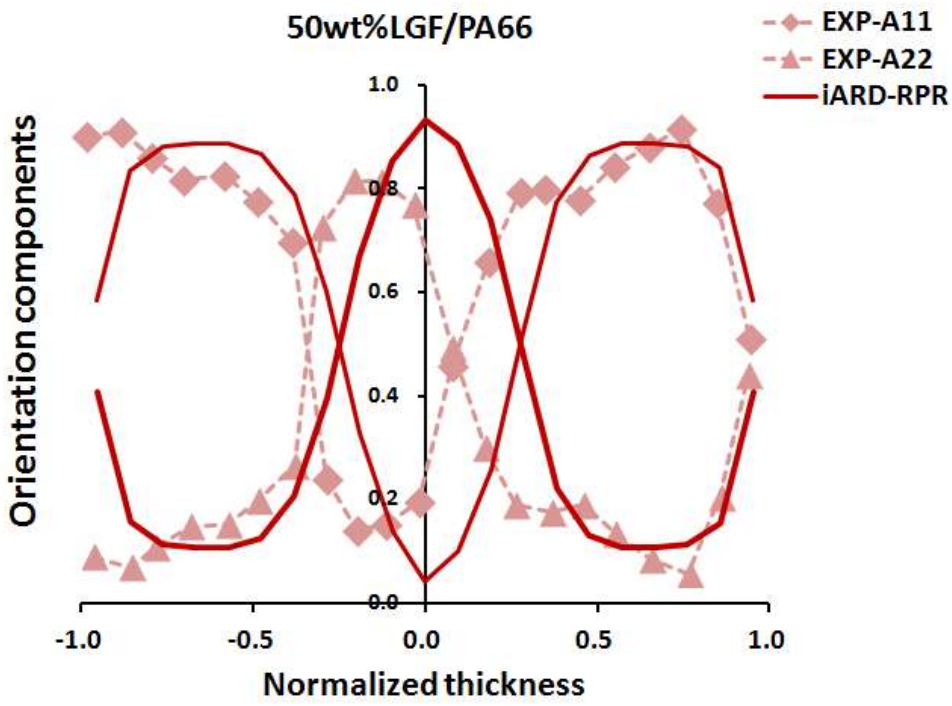

Figure 2: Comparison of the predicted orientation distributions along the flow and cross-flow directions (A11 and A22) through normalized thickness at the center of the ISO plaque with experimental validation for 50wt% LGF/PA66 (Dupont) composite.

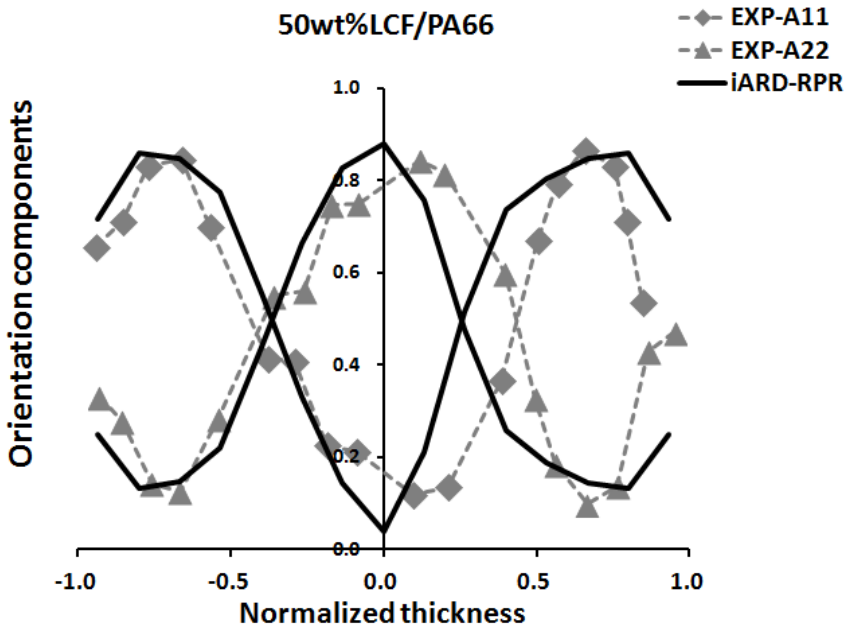

Figure 3: Comparison of the predicted orientation distributions along the flow and cross-flow directions (A11 and A22) through normalized thickness at the center of the ISO plaque with experimental validation for 50wt% LCF/PA66 (PlastiComp) composite.

II. Prediction of mechanical performance

In the foregoing section, fiber orientation predictions were performed and the results were validated with the disclosed experimental data for two injection-molded fiber thermoplastic composites. A micromechanical material modeling software, Digimat-MF, based on the Mori-Tanaka Mean Field homogenization scheme[12], was used to compute the mechanical performance of the fiber-reinforced thermoplastic composites. In the Digimat-MF computation, the fiber aspect ratio of 100 and 300 were given for the Dupont 50wt% LGF/PA66 and PlastiComp 50wt% LCF/PA66 composites, respectively. From the predicted fiber orientation distributions (**Figures 2 and 3**) in the last section, the thickness-averaged values of A_{11} and A_{22} at the center of the end-gated plaque are listed in **Table II**.

Based on these data, Digimat-MF was applied to obtain both the flow-directional and maximum modulus E_1. Consequently, the predicted modulus E_1 was about 14.6 and 43.0 GPa for the 50wt% LGF/PA66 and 50wt% LCF/PA66 composites, respectively. A further comparison was made of modulus E_1 to find: 50wt% LCF/PA66 >> 50wt% LGF/PA66.Thus, *adding a large amount of long carbon fibers to pure PA66 is more effective in enhancing the mechanical performance than with short glass fiber and long glass fiber.* Compared with the experimental bulk value of tensile modulus (E_{exp})[13-14], the predictive moduli are roughly satisfied in **Table II**. The tensile modulus and stress against strain in various fiber composites are presented in

Figure 4. Clearly, adding a large amount of long carbon fibers to pure PA66 is more effective in enhancing the mechanical performance than with long glass fiber. In addition, the stress-strain response obtained: 50wt% LCF/PA66 >> 50wt% LGF/PA66. Overall, these predictions of the reinforcing ability agree well with the related experiments.

Table II: The thickness-averaged orientation tensor components (A_{11} and A_{22}) and the predicted tensile moduli (E_1) at the center of the plaque for different materials with the aspect ratio (a_r) and the experimental bulk value of tensile modulus (E_{exp}).

Materials	a_r	A_{11}	A_{22}	E_1 (GPa)	E_{exp} (GPa)
50wt% LGF/PA66	100	0.619	0.363	14.6	18
50wt% LCF/PA66	300	0.597	0.384	43.0	40

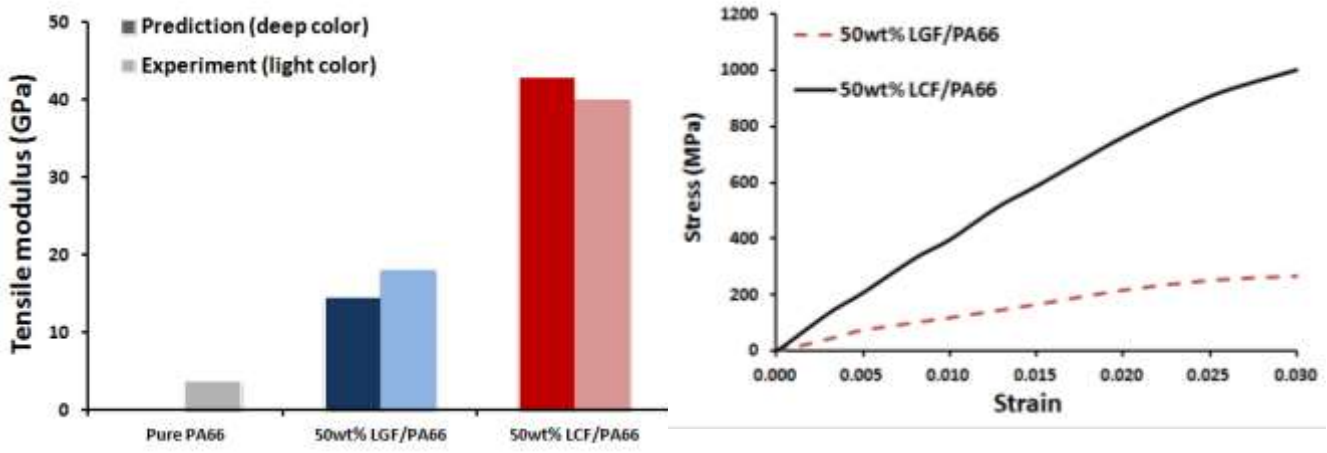

Figure 4: Tensile modulus and stress response for various fiber composites.

Conclusion

Ultimately, we have performed accurate predictions of fiber orientation in injection molding simulation of various fiber reinforced composites; the aim was to estimate reliable mechanical properties. From the simulations, the mechanical performance of the long carbon fiber reinforced PA66 is superior to that of the long glass fiber reinforced PA66. Such a predictive finding is in good correlation with the experimental results. An objective fiber orientation model plays a critical role in the accurate predictions of fiber orientation. Since the complex geometry of real automotive products involves various changes in the direction of the flow, along with the inclusion of ribs and the changes in the thickness and holes, discovering how to determine the optimal parameters of the fiber orientation model is an important challenge for future research.

Bibliography

1. Folgar F and Tucker III CL. Orientation Behavior of Fibers in Concentrated Suspensions. *J Reinf Plast Compos*. 1984; 3: 98-119.

2. Wang J, O'Gara JF and Tucker III CL. An Objective Model for Slow Orientation Kinetics in Concentrated Fiber Suspensions: Theory and Rheological Evidence. *J Rheol*. 2008; 52: 1179-1200.
3. Phelps JH and Tucker III CL. An Anisotropic Rotary Diffusion Model for Fiber Orientation in Short- and Long-Fiber Thermoplastics. *J Non-Newtonian Fluid Mech*. 2009; 156: 165-176.
4. Nguyen N, Jin X, Wang J, *et al.* Implementation of New Process Models for Tailored Polymer Composite Structures into Processing Software Packages. *the US Department of Energy, Pacific Northwest National Laboratory, PNNL Report under Contract DE-AC05-76RL01830*. 2010; PNNL-19185.
5. Tseng H-C, Chang R-Y and Hsu C-H. An Objective Tensor to Predict Anisotropic Fiber Orientation in Concentrated Suspensions. *J Rheol*. 2016; 60: 215-224.
6. Foss PH, Tseng H-C, Snawerdt J, Chang Y-J, Yang W-H and Hsu C-H. Prediction of Fiber Orientation Distribution in Injection Molded Parts Using Moldex3d Simulation. *Polym Compos*. 2014; 35: 671-680.
7. Tseng H-C, Chang R-Y and Hsu C-H. Method and Computer Readable Media for Determining Orientation of Fibers in a Fluid. *US Patent* 2013; No. 8,571,828.
8. Moldex3D. *User Manual and Material Database*. Hsinchu, Taiwan: CoreTech System, 2015.
9. Phelps JH. Processing-Microstructure Models for Short- and Long-Fiber Thermoplastic Composites. University of Illinois at Urbana-Champaign, 2009.
10. Jin X, Wang J and Han S. Long Fiber Polymer Composite Property Calculation in Injection Molding Simulation. *AIP Conference Proceedings*. 2013.
11. Nguyen BN, Fifield L, Kijewski S, *et al.* Predictive Engineering Tools for Injection-Molded Long-Carbon-Fiber Thermoplastic Composites - Fy 2015 First Quarterly Report. *the US Department of Energy, Pacific Northwest National Laboratory, PNNL Report under Contract DE-AC05-76RL01830*. 2015; PNNL-24031.
12. Papathanasiou TD and Guell DC. *Flow-Induced Alignment in Composite Materials*. Woodhead: Cambridge, 1997.
13. Lee SM. Handbook of Composite Reinforcements. New York: VCH, 1993, p. 549.
14. PlastiComp. Technical Data Sheet-50% Long Carbon Fiber/Nylon 66.